The use of electrospray ionization tandem mass spectrometry on the structural characterization of novel asymmetric metallo-organic supermolecules, based on pentafluorophenylporphyrins and ruthenium complexes

Emmanuel Zimmermman Moreira [a], Luiz Alberto Beraldo de Moraes [a], Marcos Nogueira Eberlin [b], Yassuko Iamamoto [a], Sofia Nikolaou [c,*]

[a] Departamento de Química da Faculdade de Filosofia Ciências e Letras de Ribeirão Preto, Universidade de São Paulo, Brazil
[b] Laboratório ThoMSon de Espectrometria de Massas, Instituto de Química da Universidade Estadual de Campinas, UNICAMP, Brazil
[c] Departamento de Física e Química da Faculdade de Ciências Farmacêuticas de Ribeirão Preto, Universidade de São Paulo, Av. do Café s/n, 14040-903 Ribeirão Preto, SP, Brazil

ARTICLE INFO

ABSTRACT

The novel asymmetric metallo-organic triads cis- and $trans$-[B(4-py)BPFPH$_2$\{Ru$_3$O(Ac)$_6$(py)$_2$\}\{Ru(bpy)$_2$Cl\}](PF$_6$)$_2$ (**5a,b**) for which cis- and $trans$-B(4-py)BPFPH$_2$ = 5,10-bis(pentafluorophenyl)-15,20-bis(4-pyridyl)porphyrin and 5,15-bis(pentafluorophenyl)-10,20-bis(4-pyridyl)porphyrin, respectively; Ac = acetate; py = pyridine and bpy = 2,2′-bipyridine, as well as their corresponding monosubstituted dyads cis- and $trans$-[B(4-py)BPFPH$_2$\{Ru$_3$O(Ac)$_6$(py)$_2$\}]PF$_6$ (**4a,b**) have been structurally characterized via electrospray ionization mass spectrometry (ESI-MS and ESI-MS/MS). The ESI-MS of dyads **4a,b** display two characteristic Ru-multicomponent clusters of isotopologue ions corresponding to singly charged ions **4a,b**$^+$ of m/z 1629 and doubly charged ions [**4a,b**+H]$^{2+}$ of m/z 815 and the triads **5a,b** are detected by ESI-MS as the intact doubly charged cluster of isotopologue ions of m/z 1039 [**5a,b**]$^{2+}$. The ESI-MS/MS of **4a,b**$^+$, [**4a,b**+H]$^{2+}$ and [**5a,b**]$^{2+}$ reveal characteristic dissociation pathways, which confirm the structural assignments providing additional information on the intrinsic binding strengths of the gaseous ions. Although the gas-phase behavior of each pair of isomers was rather similar, the less symmetric dyads **4a,b** are distinguished via the ^{1}H NMR spectral profile of the pyrrolic signals. Exploratory photophysical assays have shown that both modifying motifs alter the porphyrinic core emission profile, opening the possibility to use these asymmetric systems as photophysical devices.

1. Introduction

Electrospray ionization mass spectrometry (ESI-MS) as well as its tandem version (ESI-MS/MS) have been increasingly used for the structural characterization of organometallic [1], metallo-organic [2], inorganic molecules [3] and supermolecules and their ionic forms [4]. ESI is particularly suited for such species due to its ability to transfer, via an unique and gentle ion evaporation process, pre-formed ions directly from solutions to the gas phase environment of mass spectrometers [5]. ESI-MS is also advantageous for the structural characterization of organometallic and inorganic complexes owing to detailed structural information on both metal cores and ligands, isotope profiles, and high sensitivity, therefore requiring reduced amounts of sample as those required for other conventional techniques, such as NMR and cyclic voltammetry,

which are more commonly applied to characterize organometallic and inorganic complexes [6].

Regarding the compounds of interest to this work, porphyrins and metalloporphyrins are molecules of great interest particularly in chemistry, biology and physics, also featuring important industrial applications. They display useful properties such as the ability to mimic biologically-active structures like cytochrome P450 monooxygenases, to act as catalysts and as photosensitizers in photodynamic therapy [7]. Recently, ESI-MS(/MS) has been applied with success to characterize these molecules [8], as well as supramolecular extended structures based on the porphyrinic core [9].

On the other hand, μ-oxo triruthenium acetates complexes constitute a versatile class of molecules that display rich electrochemical behavior, including electrochromism, and interesting spectroscopic and catalytic properties [10]. Relevant work has been done using these triruthenium carboxylates as modifying motifs to porphyrins [11], as building blocks in extended structures which feature electron transfer reactions [12], as well as acceptors for photoinduced transfer reactions in supramolecular assemblies [13]. Their well known chemistry has recently allowed researchers to
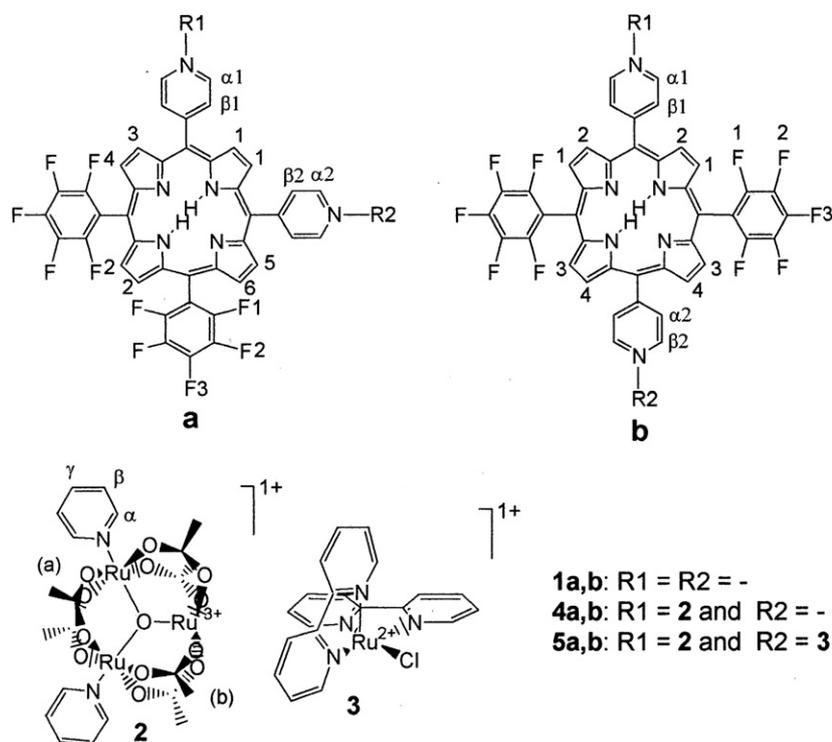
Fig. 1. Structures of the compounds studied herein and labels for NMR assignments.

plan novel clusters with important properties, such as controlled and reversible NO or CO delivery [14]. With respect to the [Ru(bpy)₃] moiety, this and related ruthenium polypyridine complexes have been extensively explored and their chemical, electrochemical and spectroscopic (photophysical) behaviors well-described in the literature [15].

This work focuses the structural characterization, via ESI-MS-(/MS) and ^{1}H and ^{19}F NMR analysis, of a series of substituted pentafluoropyridylporphyrins synthesised by a suitable approach designed in order to obtain the asymmetric metallo-organic dyads **4a,b** and triads **5a,b** (Fig. 1). It is also presented a brief spectroscopic characterization, as well as preliminary photophysical data. Usually, triads such as **5** are composed by a porphyrin central chromophore and peripheral organic electron donor and acceptor units, which are designed to mimic the active centers of the natural photosynthetic systems. Those triads are able to generate excited states of charge separation and thus convert light into chemical energy [16]. For the novel asymmetric metallo-organic systems **5a,b** that we have prepared, the ruthenium trinuclear complex **2** may act as an electron acceptor owing to its ability to participate in photoinduced electron and energy transfers [13], and the [Ru(bpy)₂] moiety **3** would act as a tunable unit able to display either the acceptor or the donating ability, depending on the experiment conditions [17].

2. Experimental

All the reactants were commercially available and used without further purification. The compounds [Ru(bpy)₂Cl₂] · 2H₂O, [Ru₃O-(Ac)₆(py)₂(CH₃OH)]PF₆ and cis- and trans-B(4-py)BPFPH₂(5,10-bis-(pentafluorophenyl)-15,20-bis(4-pyridyl)porphyrin and 5,15-bis(pentafluorophenyl)-10,20-bis(4-pyridyl)porphyrin, respectively) were synthesized according to reported procedures [18]. The description of the purification and isolation of the cis- and trans-pentafluoropyridylporphyrins isomers is detailed elsewhere [19].

2.1. Synthesis of cis- and trans-[B(4-py)BPFPH₂{Ru₃O(Ac)₆(py)₂}]PF₆ (dyads **4a,b**)

About 51.3 mg of [Ru₃O(Ac)₆(py)₂(CH₃OH)]PF₆ (5.1 × 10⁻⁵ mol) was dissolved in 70 mL of dichloromethane and the resulting solution were slowly dropped into a solution of 45 mg (5.6 × 10⁻⁵ mol) of cis- or trans-[B(4-py)BPFPH₂], dissolved in 5 mL of dichloromethane. The reaction mixture was magnetically-stirred for 24 h, at room temperature under aerobic conditions. The resulting solution was evaporated to dryness and the purple solid obtained was purified by chromatography in a neutral alumina column of approximately 20 cm high and 2.5 cm of diameter. The solvent used for elution was dichloromethane and the fractions eluted from the column were identified by their UV–Vis absorption spectra. For both dyads **4a,b**, the first fraction eluted was identified as unreacted porphyrin; the following fraction apparently contained mixtures with variable amounts of porphyrin and ruthenium complex. The third fraction contained dyads **4** and the last fraction contained the symmetric, bi-substituted triads cis- and trans-[B(4-py)BPFPH₂{Ru₃O(Ac)₆(py)₂}₂](PF₆)₂ (m/z 1229 for the cations cis- or trans-[B(4-py)BPFPH₂{Ru₃O(Ac)₆(py)₂}₂]²⁺; cis-[B(4-py)BPFPH₂{Ru₃O(Ac)₆(py)₂}₂](PF₆)₂ η = 6%; trans-[B(4-py)BPFPH₂{Ru₃O(Ac)₆(py)₂}₂](PF₆)₂ η = 9%). **4a** (η = 31); λ_max(dichloromethane)/nm (log ε/dm³ cm⁻¹ mol⁻¹ and assignment [18]) 414 (5.5, Soret), 510 (4.4, Q_{y(1,0)}), 545 (3.9, Q_{y(0,0)}), 587 (4.1, Q_{x(1,0)}), 655 (4.0, Q_{x(0,0)}) and 691 (4.0, intra-cluster). **4b** (η = 45); λ_max(dichloromethane)/nm (log ε/dm³ cm⁻¹ mol⁻¹ and assignment) 414 (5.4, Soret), 510 (4.4, Q_{y(1,0)}), 545 (3.8, Q_{y(0,0)}), 587 (4.0, Q_{x(1,0)}), 655 (3.9, Q_{x(0,0)}) and 691 (3.9, intra-cluster).

2.2. Synthesis of cis- and trans-[B(4-py)BPFPH₂{Ru₃O(Ac)₆(py)₂}{Ru(bpy)₂Cl}](PF₆)₂ (triads **5a,b**)

About 37.9 mg of dyad **4a,b** (2.1 × 10⁻⁵ mol) and 12.2 mg of [Ru(bpy)₂Cl₂] (2.5 × 10⁻⁵ mol) were dissolved in 10 mL of dichlo-

romethane and allowed to react during 48 h, under gentle heat, magnetic stirring and aerobic conditions. The reaction media was then dropped into an alcoholic saturated solution of NH_4PF_6 and, after 2 h, was evaporated to dryness, yielding a black solid. The crude material were purified by chromatography in a neutral alumina column of approximately 20 cm high and 2.5 cm of diameter; the solvent used for elution was a 1% mixture (v/v) of ethanol: dichloromethane and the fractions eluted from the column were identified by their UV–Vis absorption spectra. The products of interest were collected as the third fraction eluted from the column. **5a** (η = 30%); λ_{max}(dichloromethane)/nm (log ε/dm^3 cm^{-1} mol^{-1} and assignment) 296 (4.4, π–π^*), 417 (5.0, Soret), 511 (4.0, $Qy(1,0)$), 545 (3.7, $Q_{y(0,0)}$), 587 (3.7, $Q_{x(1,0)}$), 650 (3.4, $Q_{x(0,0)}$) and 691 (3.5, intra-cluster). **5b** (η = 6%); λ_{max}(dichloromethane)/nm (log ε/dm^3 cm^{-1} mol^{-1}and assignment) 295 (4.3, π–π^*), 416 (4.8, Soret), 512 (3.9, $Qy(1,0)$), 548 (3.5, $Q_{y(0,0)}$), 588 (3.6, $Q_{x(1,0)}$), 650 (3.4, $Q_{x(0,0)}$) and 690 (3.4, intra-cluster).

2.3. Physical measurements

The mass spectrometric experiments were performed using a high-resolution hybrid quadrupole (q) and orthogonal time-of-flight (TOF) mass spectrometer (QTOF from Waters Micromass, UK) operating in the positive ion mode at ca. 5000 resolving power. The temperature of the nebulizer was 150 °C and the cone voltage was 30 V. The ESI-MS/MS experiments were performed via Q1 selection of the ion or cluster of ions of interest followed by collision-induced dissociation (CID) with argon in the collision hexapole at energies ranging from 10 to 20 eV and TOF-MS analysis of the ionic fragments. Samples were dissolved in a 1:1 methanol/water solution acidified by the addition of 0.1% formic acid. The ^{1}H, COSY (^{1}H–^{1}H, not shown) and ^{19}F NMR data were collected on a Bruker Advanced DRX 400MHz spectrometer (Bruker Biospin, Bremen, Germany), from 1×10^{-2} mol dm^{-3} CDCl$_3$ solutions. The electronic spectra were recorded on a HP 8453 spectrophotometer, from 1×10^{-5} mol dm^{-3} dichloromethane solutions. Steady-state emission and excitation spectra were recorded on a Spex Fluorolog 2 spectrophotometer (excitation slit = 10 and emission slit = 20), at room temperature in a four faced 1 cm × 1 cm quartz cuvette, from approximately 5×10^{-6} mol dm^{-3} degassed dichloromethane solutions. The quantum yields were calculated from degassed CH$_2$Cl$_2$ solutions, using the known value of ϕ_s for TPPH$_2$ (tetraphenyl porphyrin) at room temperature (ϕ_s = 0.099) and the integrated areas under the emission curve corrected by the relative absorbance at the excitation wavelength [17a,20].

3. Results and discussion

3.1. Synthesis

Obtaining the monosubstituted dyads **4a,b** is not a trivial task, since both coordination sites of the precursor isomers **1a,b** (the pyridyl group) are equivalent. Nevertheless, the synthetic approach proposed here is based on the use of sub-stoichiometric amounts of the modifying motif (in this case the trinuclear ruthenium complex **2**), and the addition of a diluted solution of the complex to a more concentrated solution of the porphyrinic core, in order to warranty local excess of porphyrin. Besides that, the reaction was submitted to soft conditions (room temperature and magnetic stirring), and care was taken not to extend the reaction too long, minimizing it to further yield high quantities of the bisubstituted product. This synthetic strategy, along with the adsorption chromatography purification, allowed one to obtain the monosubstituted dyads (η = 31% and η = 45% for **4a** and **4b**, respectively) in higher yield, although the coordination of two trinuclear com-

plexes molecules to the central core has occured to some extent, yielding smaller amounts of the bisubstituted symmetric byproduct, which was collected as the last fraction from the chromatographic column.

In the particular case of compounds **5a,b**, once one of the coordination sites of the porphyrinic center was already compromised with the bond to complex **2**, there was no need to have a rigid control on the synthetic conditions, and the asymmetric triads were obtained by the use of a slight excess of the [Ru(bpy)$_2$] substituent and a more concentrated reaction medium.

3.2. ESI-MS(/MS)

The porphyrins **1a,b** as well as the dyads **4a,b** and triads **5a,b** show nearly identical gas-phase behaviour, therefore we will comment only on the ESI-MS results for the *cis*-isomers (a). ESI-MS detects the model *cis*-porphyrin **1a** as a cluster of singly-charged mono-protonated molecule [**1a**+H]$^+$ of *m/z* 797 (only the *m/z* of the most intense ion within the isotope cluster will be mentioned). Note that mono-protonation may occur either on a central N atom of the porphyrin ring or on an N hetero-atom of the pyridyl groups. The cluster from the doubly protonated molecule [**1a**+2H]$^{2+}$ of *m/z* 398.5 was not observed at all, indicating that the addition of a second proton to the porphyrin molecule is unfavourable, at least for the gaseous molecule. The gaseous [**1a**+H]$^+$ of *m/z* 797 was then selected and dissociated via 20 eV collisions with argon (spectrum not shown). Interestingly, dissociation occurs to great extent by several successive losses of HF molecules (20 Da). These sequential losses must therefore require substantial molecular rearrangements that are accessed likely due to the lack of alternative less energy-demanding direct bond cleavages.

The ESI-MS of the model compound [Ru$_3$O(Ac)$_6$(py)$_2$-(CH$_3$OH)]PF$_6$, that is **2** · PF$_6$, display a multicomponent cluster of isotopologue ions of *m/z* 863 mostly characteristic of the Ru$_3$ composition (ruthenium is a multiple isotope element: ^{104}Ru (18.7%), ^{102}Ru (31.6%), ^{101}Ru (17.0%), ^{100}Ru (12.6%), ^{99}Ru (12.7%), ^{98}Ru (1.88%) and ^{96}Ru (5.52%)). This ion is ascribed to the methanol adduct of **2**$^+$ (Fig. 2) that is, [Ru$_3$O(Ac)$_6$(py)$_2$(CH$_3$OH)]$^+$. This whole isotopologue cluster of singly charged ions was therefore selected and subjected to 20 eV collision induced dissociation (CID). Extensive CID occurs (Fig. 2) yielding first [Ru$_3$O(Ac)$_6$(py)$_2$]$^+$ of *m/z* 831, that is **2**$^+$. This preferential loss of methanol over pyridine is consistent with the binding strength of both ligands, that is, also in gas phase methanol is more loosely bonded to Ru than py, mimicking the solution behaviour [3]. After methanol loss, successive losses of the two more strongly bonded pyridine ligands (py) occurs thus yielding the fragment ions of *m/z* 751 and *m/z* 672, which are assigned, respectively to [Ru$_3$O(Ac)$_6$py]$^+$ and [Ru$_3$O(Ac)$_6$]$^+$. The fragment ion of *m/z* 751 dissociates further by an unexpected and interesting process that involves the loss of four acetate (Ac) ligands. We rationalize this dissociation by the release of two neutral dimeric molecules of Ac$_2$ composition, thus yielding the [Ru$_3$O(Ac)$_2$(py)]$^+$ fragment of *m/z* 516. This fragment ion fragments further by pyridine loss to form [Ru$_3$O(Ac)$_2$]$^+$ of *m/z* 437.

The ESI-MS of the acidified water:methanol solution of dyad **4a** (spectrum not shown) displays predominantly two prominent clusters of isotopologue ions of similar abundances. In one cluster of *m/z* 1629, the ions are separated by one *m/z* unit indicating that they are singly charged species, ascribed therefore to **4a**$^+$. The other of *m/z* 815 displays ions separated by 1/2 *m/z* unit, and is ascribed to the mono-protonated and therefore doubly charged ion [**4a**+H]$^{2+}$. Fig. 3 shows the ESI-MS/MS of both **4a**$^+$ and [**4a**+H]$^{2+}$.

The gaseous **4a**$^+$ of *m/z* 1629 (Fig. 3a) dissociates promptly upon 20 eV collisions with argon by sequential losses of the peripheral pyridine ligands, yielding the cluster of isotopologues singly-charged ions [**4a**-py]$^+$ and [**4a**-2py]$^+$ of *m/z* 1550 and *m/z* 1471,
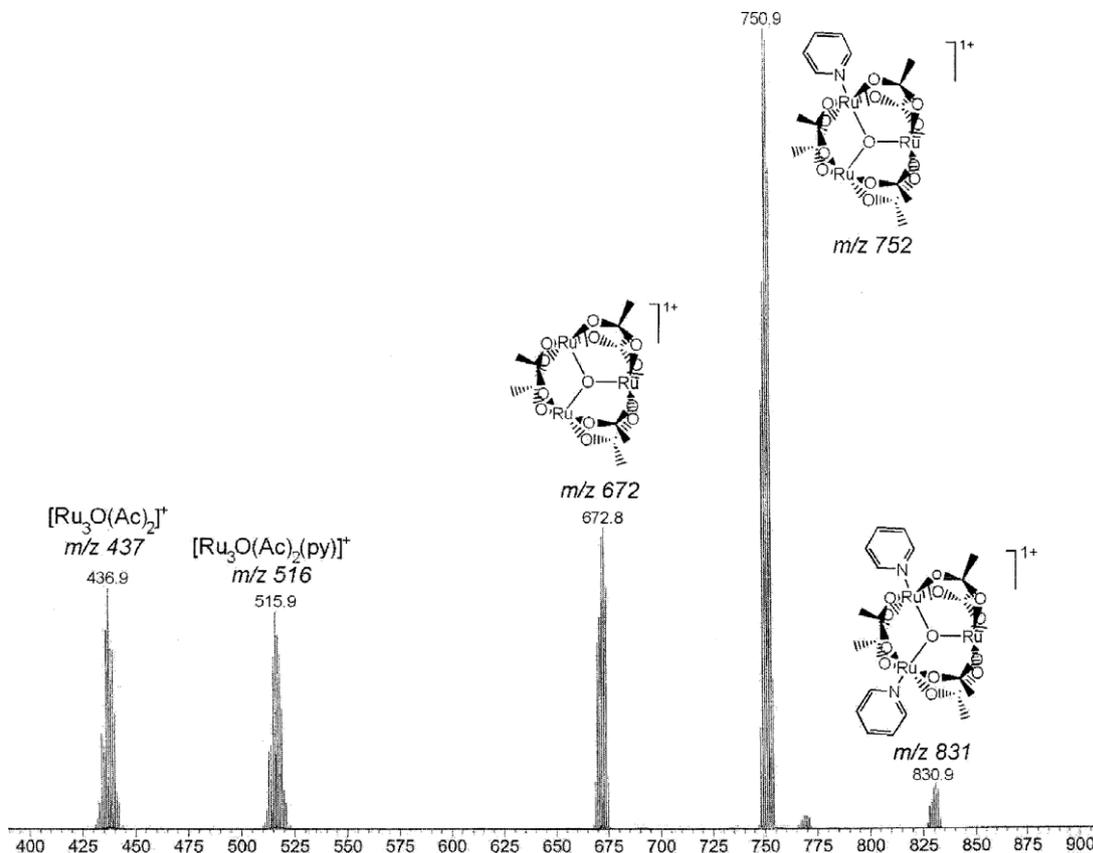
Fig. 2. ESI-MS/MS for 20 eV CID of $[Ru_3O(Ac)_6(py)_2]^+$ of m/z 831. Proposed structures and dissociation pathways for the fragment ions are shown as inserts. The parent species $[Ru_3O(Ac)_6(py)_2(CH_3OH)]^+$ of m/z 863 dissociates completely and is not detected.

respectively. It dissociates also to form the isotopologue cluster of 2^+ ions of m/z 831 due to the loss of the entire porphyrin ligand hence due to the dissassembly of the supramolecular dyad. It was previously reported [9c] that for a similar supramolecular system in which a tetra-pyridyl porphyrin is modified exclusively with the $[Ru(bpy)_2Cl]$ fragment, CID fails to form supramolecular species via the loss of peripheral 2,2′-bipyridine ligand (a fragment that would be analogous to $[4a-py]^+$). Instead, only the successive cleavage of the Ru–pyridyl bond was observed thus yielding the two fragments composing the supermolecular assembly. For that assembly, the chelate effect stabilizes the Ru–bpy bond making it stronger than the Ru–pyridyl bond. For $4a^+$ however, we observe a different behaviour: the three fragments and their relative abundances, $[4a-py]^+ > [4a-2py]^+ = [2]^+$ and the absence of any additional effect such as the chelate one lead us to conclude that at least for the unprotonated $4a^+$ species, the bond of the $[Ru_3O]$ core to the porphyrin through the pyridyl group (the one that sustain the supramolecular assembly), is as strong as the bond of the $[Ru_3O]$ to the peripheral pyridine ligands.

In Fig. 3a we also observe that $4a^+$ of m/z 1629 dissociates to form a cluster of singly charged (separated by one m/z unit) isotopologue ions of m/z 752, which corresponds to $[2-py]^+$. Being the most abundant fragment ion, we assume that probably $[2-py]^+$ is originated not solely from 2^+ of m/z 831, but also from $[4a-py]^+$ of m/z 1550. Further fragmentation of $4a^+$ also occurs to originate less abundant ions such as $[Ru_3O(Ac)_2py]^+$ and $[Ru_3O(Ac)_2]^+$ of m/z 516 and m/z 437, respectively.

The ESI-MS/MS of the isotopologue cluster of $[4a+H]^{2+}$ ions of m/z 815 is quite unique and illustrative (Fig. 3b). It shows that the ion loses the peripheral pyridine ligand of 89 Da to form the doubly charged cluster of supramolecular species $[4a+H-py]^{2+}$ of m/z 775, separated by 1/2 m/z units. This loss reinforces the indica-

tion that the Ru–porphyrin bond is quite strong. Due to pyridyl–Ru bond cleavage, $[4a+H]^{2+}$ of m/z 815 also dissociate by "charge partitioning" to form two singly charged species: the singly charged cluster of isotopologue ions $[1a+H]^+$ of m/z 797 (with a much less diverse isotope pattern) and 2^+ of m/z 831 (a diverse Ru_3-isotope pattern) both containing ions separated by one m/z unit. Note that 2^+ undergoes further dissociation by the loss of one peripheral pyridine, yielding the cluster of singly charged isotopologue ions $[2-py]^+$ of m/z 752.

The ESI-MS of the triad $5a$ solution shows that ESI is able to gently transfer to the gas phase the doubly charged ion $5a^{2+}$ of m/z 1039 with spatially separated charge sites, detecting it unambiguously as a characteristic cluster of isotopologue ions separated by 1/2 m/z unit. The ESI-MS data shows therefore that the synthetic approach reported herein to obtain the assymmetrical $5a,b$ isomeric supermolecules was successful. To obtain structural confirmation for $5a$, and for clarity and illustration, the ESI-MS/MS of the ions of m/z 1039 (in fact a mixture of isobaric Ru-isotopologue ions) selected from the multicomponent cluster of isotopologue ions of $5a^{2+}$ (see inset) was acquired (Fig. 4). Scheme 1 depicts the "charge partitioning" dissociation pattern proposed for $5a^{2+}$.

The doubly charged $5a^{+2}$ ions of m/z 1039 dissociates mainly by "charge partitioning" to yield two pairs of singly charged cations, that is, (i) $4a^+$ of m/z 1630 and $[B(4-py)BPFPH_2\{Ru(bpy)_2Cl\}]^+$ of m/z 1247 and (ii) 2^+ of m/z 833 and 3^+ of m/z 449. The fragment $4a^+$ undergoes further dissociation by the loss of its peripheral pyridine ligand to yield $[4a-py]^+$ of m/z 1551.

3.3. NMR spectroscopy

Table 1 summarize the tentative assignment of the observed NMR signals for $1a,b$ (^1H and ^{19}F) and $4a,b$ (^1H). ^{19}F-RMN spectra

a

m/z 752

752.9

[Ru₃O(Ac)₂(py)]⁺
m/z 516

[Ru₃O(Ac)₂]⁺
m/z 437

435.9

518.9

m/z 673
674.8

m/z 831
833.9

m/z 1471
1473.1

m/z 1550
1550.2

200   400   600   800   1000   1200   1400   1600   1800   2000   2200   2400

b

797.2

m/z 797

m/z 775
775.5

m/z 831
830.9

m/z 752
753.9

815.1

745   750   755   760   765   770   775   780   785   790   795   800   805   810   815   820   825   830   835
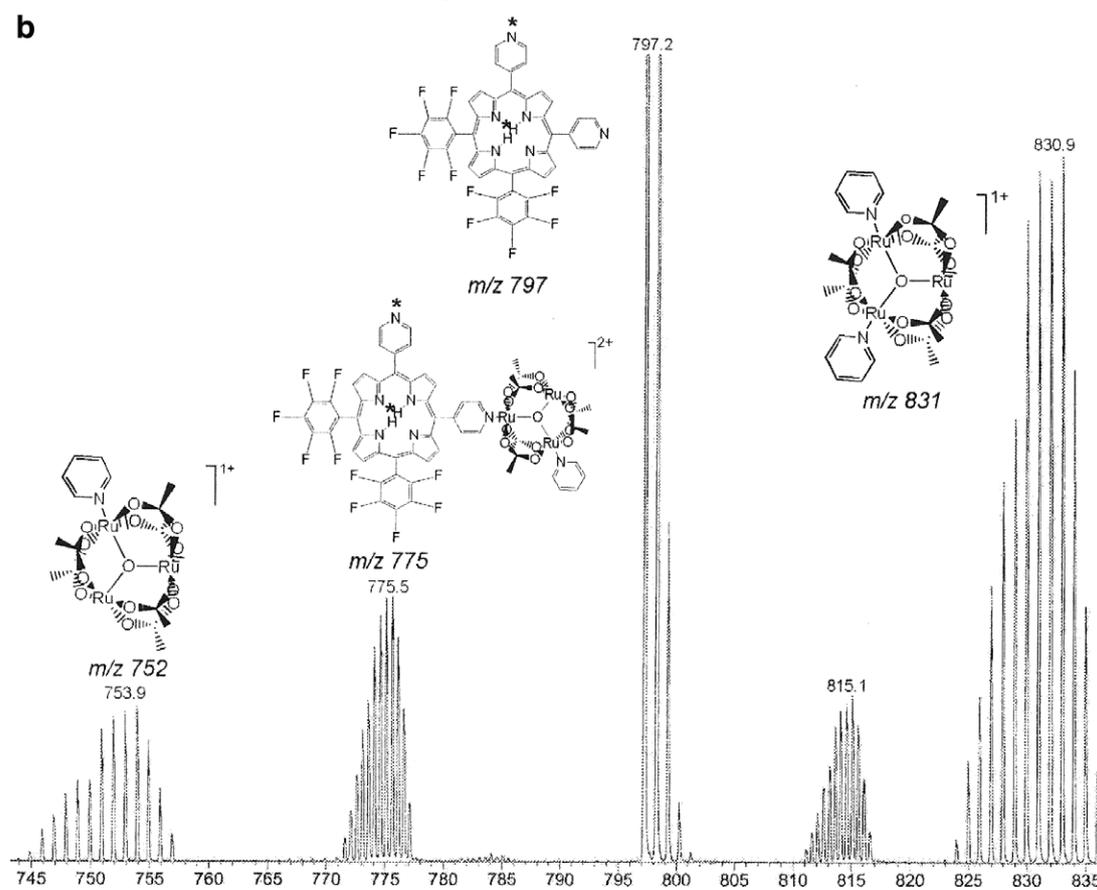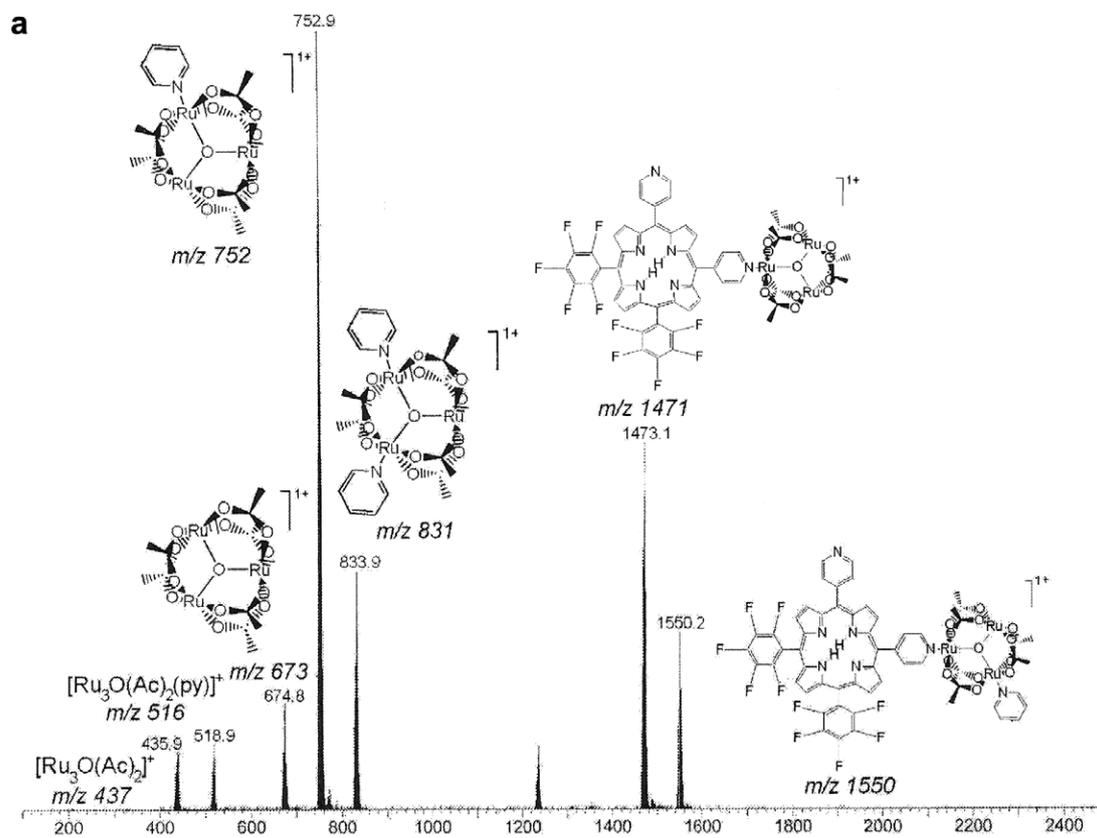
Fig. 3. ESI-MS/MS for 20 eV CID of: (a) **4a**⁺ of *m/z* 1629 and (b) [**4a**+H]²⁺ of *m/z* 815.
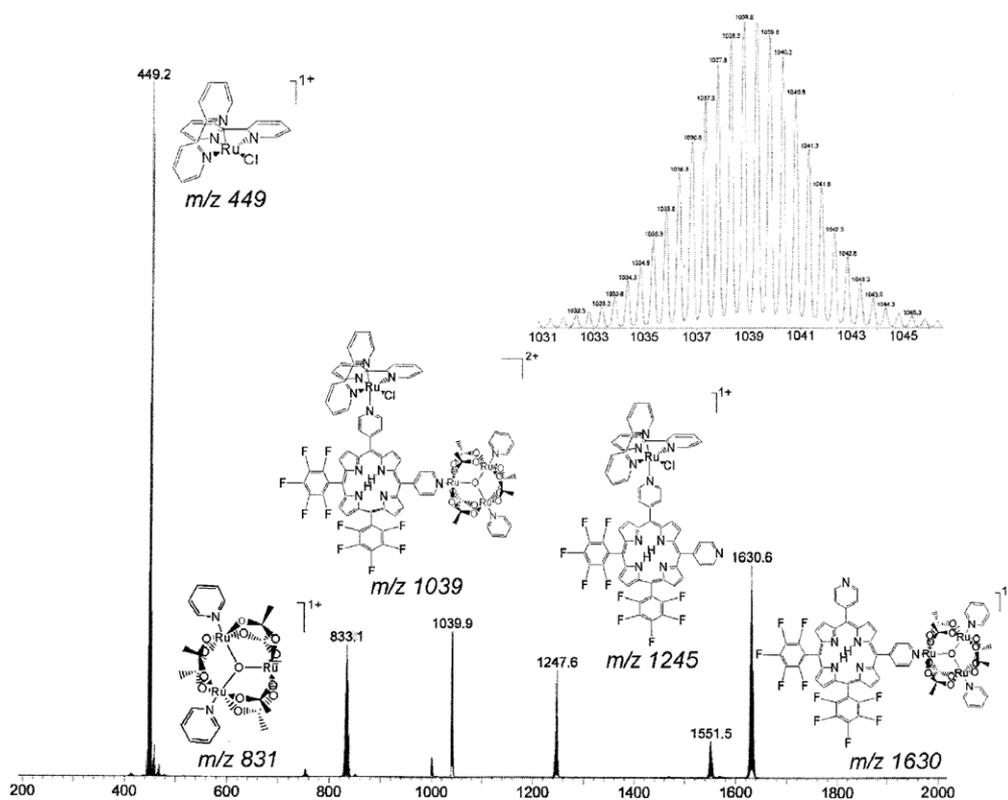
Fig. 4. ESI-MS/MS for 15 eV CID of **5a**$^{2+}$ of m/z 1039. The inset shows the full cluster of isotopologue ions of **5a**$^{2+}$ detected by ESI-MS.

are quite useful to characterize fluorinated porphyrins [21]. As expected for isomers **1a** and **1b**, the ^{19}F-RMN spectra display three sets of signals corresponding to the *ortho*, meta and *para* fluorines. Each signal appears as a doublet and two triplets, respectively, and show no significant variations on the chemical shifts values between the *cis* to the *trans* isomer. The pyrrolic ^{1}H signals of the *cis*-porphyrin isomer 1, however, which were expected to appear as a set of two doublets and two singlets [22], are superimposed into two distorted doublets, each of them integrating to four protons. This spectral profile almost converges to the one observed for the *trans* isomer 1b (two doublets), making it hard to identify the precursors isomers by the ^{1}H NMR spectra. Nevertheless, the coordination of **2** to one pyridyl position of the *cis* and *trans*-dyads **4a,b** lowers the molecular symmetry, leading to different patterns of resonances in the aromatic region of the ^{1}H spectra, making therefore the isomers distinguishable.

Concerning the [Ru$_3$O(Ac)$_6$(py)$_2$] moiety, the δ values follow the pattern dictated by the paramagnetic anisotropy of the [Ru$_3$O] core, which contains one unpaired electron [6c,10]. For the ^{1}H spectra, this effect promotes large shifts to higher field on the pyridinic protons α, β, γ, α1 and β1, which tend to vanish with distance, suggesting that the pseudo-contact is the main paramagnetic interaction mechanism operating in these molecules.

3.4. Absorption spectra and exploratory photophysical essays

In terms of the absorption spectra of dyads **4a,b** and triads **5a,b**, the coordination of the ruthenium complexes to the precursors **1a,b** causes very little perturbation on the spectra profiles, resulting in spectra which are a summation of the bands observed in the electronic spectra of each building block that composes the supermolecules (see Section 2 for λ_{max} and assignments).

Exciting isomers **1a,b** in one of their Q band leads to the typical porphyrin emission, centered around 645 and 705 nm, assigned to a fluorescence band with vibrational structure ($Q_{0,0}$ and $Q_{0,1}$ respectively, Table 2) [23]. In spite of the absorption spectra suggest poor electronic coupling among the units composing the supermolecules, going to dyads **4a,b**, one can observe that the coordination of the triruthenium compound **2** to porphyrins **1a,b** leads to a significant decrease in the fluorescence quantum yield (ϕ) and the rise of another emission band, with very low intensity, centered at 770 nm. The coordination of the second substituent (compound **3**), yielding triads **5a,b** leads to a further decrease of ϕ, but do not introduce any modification on the spectra profile.

Although it was not possible to do a selective excitation, due to band overlap in the UV–Vis spectra, triads **5a,b** were excited at 490 nm (approximately the λ_{max} of the [Ru(bpy)$_2$] MLCT transition) and neither emission from the ruthenium chromophore nor an increase in the ϕ values of the porphyrin emission were observed. In fact, the excitation spectra (not shown) were recorded monitoring all the three observed emission bands, and in all cases the spectra reproduces exclusively the spectral profile of the porphyrin (Soret and four Q bands). This result, and the low emission quantum yield observed for the supermolecules show that there is no contribution from electronic levels of the peripheral units to the porphyrin emission and that these units are quenching that emission. In the particular case of the 770 nm band, it has been assigned to a porphyrin phosphorescence [23], which might appear when there is direct sensitization of the porphyrin triplet state by energy transfer, or when the rate of intersystem crossing (ISC) is high [24]. The absence of any bands of the **2** and **3** units in the excitation spectra of triads **5a,b** excludes the first argument exposed above. Therefore, it seems that the coordination of two ruthenium compounds to the porphyrinic core has simply favored ISC by the heavy atom effect. This explanation also holds for dyads **4a,b**.

m/z 1039

m/z 449

m/z 1629

m/z 1550

m/z 1245

m/z 831
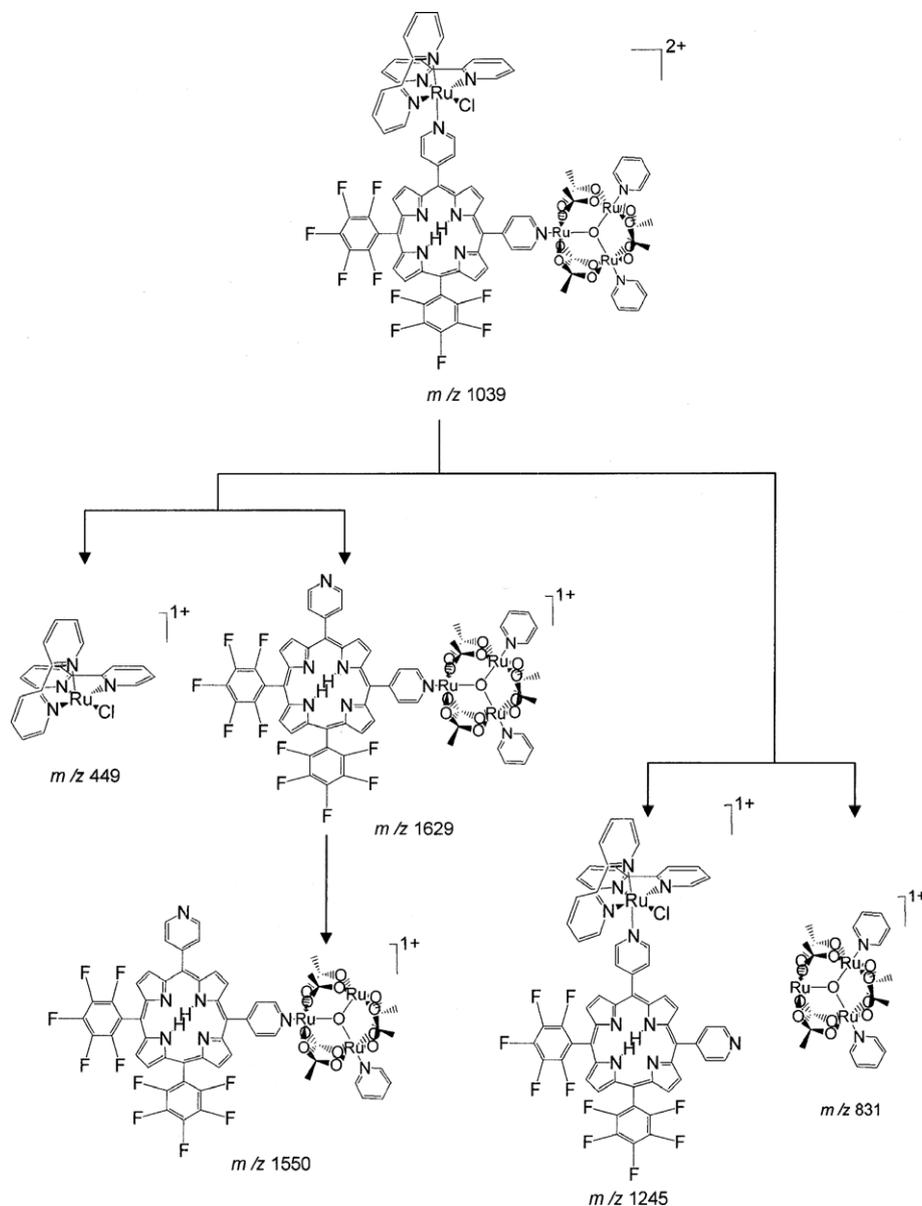
Scheme 1. Dissociation pattern of triad **5a**.

On a qualitative basis, the preliminary data presented here allows one to point out some interesting aspects: concerning the triruthenium compound **2**, it could quench the porphyrin fluorescence by a reabsorption interference, since it has an absorption band centered around 690 nm, which matches the emission bands at 650 nm/710 nm. However, there are a few literature examples in which the triruthenium compound is able to quench a [Ru(bpy)$_2$] chromophore by both photoinduced energy and electron transfers [13a] and quench Zn porphyrins and Zn phtalocyanines by photoinduced electron transfer mechanism [13c,25]. Therefore, in the present case it is possible to propose that the porphyrinic core emission is partially quenched by an electron transfer to the triruthenium moiety.

For triads **5a,b** there is the additional effect of the [Ru(bpy)$_2$Cl] modifying complex. The porphyrin singlet state might be transferring excitation energy to the MLCT[3] (metal to ligand charge transfer) of the metal complex, since the energy of this state [15b] is close to that of the emitting state of the porphyrinic core. If this is so, one would expect to detect the emission of the [Ru(bpy)$_2$Cl]

chromophore. However, in the particular case of ruthenium–bipyridine complexes whose coordination sphere is completed with a chloro ligand, the MLCT[3] is normally quenched by a low lying d–d state, which decays by non-radiative (vibrational) pathways [15b,26]. In all cases, the existence of a phosphorescence band, which arises from an ISC process, also contributes to the decrease of the porphyrin ϕ_{fl}.

Finally, although it was demonstrated here that the electronic coupling of the units which composes compound **4a,b** and **5a,b** is rather low, it is worth mentioning that, as far as we consider the present data, it seems that the difference in the position of the coordinating pyridyl groups on the porphyrinic core does not disturb the electronic properties of the molecules under investigation. Consequently, it was not detected significant differences in the spectroscopic behaviour of the isomers studied. Yet, the positional isomerism is manifested in the NMR measurements results for compounds **1a,b** and **4a,b**, since the symmetry of molecules might be directly addressed by this technique.

Table 1
Tentative assignment of the observed ^1H and ^{19}F chemical shifts (δ/ppm) for compound **1a,b** and **4a,b** from 1×10^{-2} mol dm^{-3} CDCl$_3$

	1a	1b	4a	4b
_1H_				
H1	8.92, 4H, m[a]	8.92, 4H, d	8.81, 2H, br	8.65, 2H, d
H2	≡H1	≡H1	8.76, 2H, br	8.83, 2H, d
H3	≡H1	8.86, 4H, d	≡ H2	8.16, 2H, d
H4	8.86, 4H, m	≡H3	8.19, 1H, br	8.77, 2H, d
H5	≡H4		8.65, 2H,br	
H6	≡H4		8.13, 1H, br	
H7	≡H4		≡ H5	
Inner H	−2.88, 2H, s	−2.92, 2H, s	−3.15, s	−3.20, 2H, s
Hα1	9.08, 4H, d	9.08, 4H, d	1.28, br	1.24, 2H, br
Hβ1	8.16, 4H, d	8.18, 4H, d	6.59, br	6.56, 2H, br
Hα$_2$	≡α1	≡α1	9.03, d	9.02, 2H, d
Hβ$_2$	≡β1	≡β1	8.04, d	8.08, 2H, d
Hα			0.19, br	0.12, 4H, br
Hβ			5.69, br	5.67, 4H, br
Hγ			6.34, t	6.35, 2H, t
CH$_3$ (a)			5.16, s	5.19, 6H, s
CH$_3$ (b)			5.04, s	5.06, 12H, s
_19F_[b]				
F1	−140.32, d	−141.49, d		
F2	−165.15, m	−165.18, m		
F3	−155.23, t	−155.22, t		

[a] m = multiplet, s = singlet, d = doublet, t = triplet and br = broad signal.
[b] CF$_3$C$_6$H$_5$ was used as internal standard in CDCl$_3$ solution; to facilitate comparison with the literature data [21], the reported values were converted to a scale based on the residual signal of CFCl$_3$ by summing −63, 72 ppm.

Table 2
Photophysical data for compounds **1a,b**; **4a,b** and **5a,b**[a]

	λ_{emi} (nm)	λ_{exc} (nm)	ϕ[b]
1a	647, 707	510	0.035
1b	643, 707	510	0.046
4a	647, 705, 770	510	0.0014
4b	646, 708, 770	510	0.0010
5a	649, 712, 770	510	0.00061
5b	648, 709, 770	510	0.00062

[a] Data collected from CH$_2$Cl$_2$ degassed solutions at room temperature.
[b] Fluorescence quantum yield.

4. Conclusions

Using ESI-MS and ESI-MS/MS, we have been able to gently transfer to the gas phase the corresponding cationic species **4a,b**$^+$ and **5a,b**$^{2+}$ present in solutions of dyads **4a,b** and triads **5a,b**, respectively. Using ESI-MS/MS and by performing CID of isolated gaseous ions, and by following changes in characteristic isotope patters and charge states, we have been able to characterize these gaseous ions via their structurally diagnostic dissociation chemistries. The ESI-MS(/MS) data, besides demonstrating the success of the synthetic approach used to prepare dyads **4a,b** and assymmetric triads **5a,b**, shows that these species constitute another series of gaseous ions with stable, long-lived supramolecular assemblies. The molecular _cis_ or _trans_ conformation of these species has been found to have no particular effect on their intrinsic dissociation chemistry. Via ESI-MS/MS, it was also possible to access information on the relative bond strengths of these supermolecular ions. For the singly charged dyads **4a,b**$^+$, no significant differences were observed for the cleavage of the Ru–pyridine bond or the Ru–pyridyl bond, showing that the supramolecular arrangement is supported by a strong coordinative bond. However, as expected for the doubly charged triad ions **5a,b**$^{2+}$, no preferential cleavage of the Ru–pyridyl bond was observed as opposed to the Ru–bipyridine bond, which is stabilized by the chelate effect, being thus stronger than the interaction that keeps the integrity of the triads.

Regarding the photophysical behaviour of triads **5a,b**, any further comments based on the data presented here would be too speculative. Nevertheless, this work has shown that the coordination of the triruthenium compounds do quench the porphyrin luminescence, thus acting as a final acceptor of excitation energy. Under the conditions investigated here, the [Ru(bpy)$_2$Cl] unit is also playing the function of excitation energy acceptor. Measurements at low temperature and different solvents are underway in our laboratories in order to evaluate if variations in experimental conditions would lead to a system where the [Ru(bpy)$_2$] unit would act as a donor of excitation energy and also to get a better understanding on the mechanisms of the porphyrin luminescence quenching by the substituents **2** and **3**.

References

[1] (a) C. Chevrin, J. Le Bras, A. Roglans, D. Harakat, J. Muzart, New J. Chem. 31 (1) (2007) 121;
(b) P. Wang, G.R. Newcome, C. Wesdemiotis, Int. J. Mass Spectrom. 255 (2006) 86.
[2] O. Bortolini, V. Conte, Mass Spectrom. Rev. 25 (5) (2006) 724.
[3] M.N. Eberlin, D.M. Tomazela, K. Araki, A.D.P. Alexiou, A.L.B. Formiga, H.E. Toma, S. Nikolaou, Organometallics 25 (13) (2006) 3245.
[4] (a) H.E. Toma, S. Nikolaou, M.N. Eberlin, D.M. Tomazela, Polyhedron 24 (2005) 731;
(b) F.C. Gozzo, L.S. Santos, R. Augusti, C.S. Consorti, J. Dupont, M.N. Eberlin, Chem. Eur. J. 10 (2004) 6187;
(c) M. Vazquez, M.R. Bermejo, M. Licchelli, A.M. Gonzalez-Nova, R.M. Pedrido, C. Sangregorio, L. Sorace, A.M. Garcia-Deibe, J. Satunartin, Eur. J. Inorg. Chem. (2005) 3479.
[5] (a) A.E.M. Crotti, R.L. Vessecchi, J.L.C. Lopes, N.P. Lopes, Quím Nova 29 (2) (2006) 287;
(b) R.B. Cole, in: Electrospray Mass Spectrometry, John Wiley, New York, 1997;
(c) R. Colton, A. D'Agostino, J.C. Traeger, Mass Spectrom. Rev. 14 (1995) 79.
[6] (a) M. Zamora, S. Herrero, J. Losada, I. Cuadrado, C.M. Casado, B. Alonso, Organometallics 26 (10) (2007) 2688;
(b) J.L. Vera, F.R. Roman, E. Melendez, Bioinorg. Med. Chem. 14 (24) (2006) 8683;
(c) S. Nikolaou, M. Uemi, H.E. Toma, Spec. Lett. 3 (3) (2001) 267.
[7] (a) F.S. Vinhado, P.R. Martins, A.P. Masson, D.G. Abreu, E.A. Vidoto, Y. Iamamoto, O.R. Nascimento, J. Mol. Catal. A: Chem. 188 (2002) 141;
(b) M.A. Schiavon, L.S. Iwamoto, A.G. Ferreira, Y. Iamamoto, M.V.B. Zanoni, M.D. Assis, J. Braz. Chem. Soc. 11 (2000) 458;
(c) C.M.C.P. Manso, E.A. Vidoto, H.C. Sacco, J.R. Lindsay-Smith, P.R. Martins, A.G. Ferreira, Y. Iamamoto O.R. Nascimento, J. Mol. Catal. A: Chem. 150 (1999) 141;
(d) K. Lang, J. Mosinger, D.M. Wagnerová, Coord. Chem. Rev. 248 (3–4) (2004) 321.
[8] (a) R.A. Izquierdo, C.M. Barros, M.G. Santana-Marques, A.J. Ferrer-Correia, E.M.P. Silva, F. Giuntini, M.A.F. Faustino, J.P.C. Tome, A.C. Tome, A.M.S. Silva, C.P.M.S. Neves, J.A.S. Cavaleiro, A.F. Peixoto, M.M. Pereira, A.A.C.C. Pais, J. Am. Soc. Mass Spectrom. 18 (2) (2007) 218;
(b) E.M.P. Silva, V.V. Serra, A.O. Ribeiro, J.P.C. Tome, P. Domingues, M.A.F. Faustino, M.G.P.M.S. Neves, A.C. Tome, J.A.S. Cavaleiro, A.J. Ferrer-Correia, Y. Iamamoto, M.R.M. Domingues, Rapid Commun. Mass Spectrom. 20 (23) (2006) 3605;
(c) K.S.F. Lau, M. Sadilek, G.E. Khalil, M. Gouterman, C. Bruckner, J. Am. Chem. Soc. Mass Spectrom. 16 (12) (2005) 1915.
[9] (a) K. Kano, H. Kitagishi, C. Dagallier, M. Kodera, T. Matsuo, T. Hyashi, Y. Hisaeda, S. Hirota, Inorg. Chem. 45 (11) (2006) 4448;
(b) T. Haino, T. Fujii T, Y. Fukazawa, J. Org. Chem. 71 (7) (2006) 2572;
(c) D.M. Tomazela, F.C. Gozzo, I. Mayer, R.M. Engelmann, K. Araki, H.E. Toma, M.N. Eberlin, J. Mass Spectrom. 39 (10) (2004) 1161;

(d) S. Arai, S. Ishihara, S. Takeoka, H. Ohkawa, T. Shibue, H. Nishide, Rapid Commun. Mass Spectrom. 18 (18) (2004) 2065.

[10] H.E. Toma, K. Araki, A.D.P. Alexiou, S. Nikolaou, S. Dovidauskas, Coord. Chem. Rev. 219–221 (2001) 187.

[11] (a) H. Winnischofer, V.Y. Otake, S. Dovidauskas, M. Nakamura, H.E. Toma, K. Araki, Electrochim. Acta 49 (22–23) (2004) 3711;
(b) S. Dovidauskas, H.E. Toma, K. Araki, H.C. Sacco, Y. Iamamoto, Inorg. Chim. Acta 305 (2) (2000) 206.

[12] (a) B.J. Lear, S.D. Glover, J.C. Salsman, C.H. Londergan, C.P. Kubiak, J. Am. Chem. Soc. 129 (2007) 12772;
(b) H.E. Toma, S. Nikolaou, J. Chem. Res. (S). (2000) 326;
(c) H. Kido, H. Nagino, T. Ito, Chem. Lett. (1996) 745.

[13] (a) S. Nikolaou, H.E. Toma, J. Chem. Soc., Dalton Trans. (2002) 352;
(b) H. Kunkely, A. Vogler, Inorg. Chem. Commun. 4 (2001) 689;
(c) M. Otake, M. Itou, Y. Araki, O. Ito, H. Kido, Inorg. Chem. 44 (23) (2005) 8581.

[14] (a) S. Ye, W. Zhou, M. Abe, T. Nishida, L. Cui, K. Uosaki, M. Osawa, Y. Sasaki, J. Am. Chem. Soc. 126 (24) (2004) 7434;
(b) M. Itou, Y. Araki, H. Kido, Inorg. Chem. 45 (16) (2006) 6114.

[15] (a) V. Balzani, G. Bergamini, F. Marchioni, P. Ceroni, Coord. Chem. Rev. 250 (11–12) (2006) 1254. and references cited therein;
(b) A. Juris, V. Balzani, F. Barigelletti, S. Campagna, P. Belser, A. Vonzelewsky, Coord. Chem. Rev. 84 (1988) 85.

[16] (a) G. Kodis, Y. Terazono, P.A. Liddell, J. Andreasson, V. Garg, M. Hambourger, T.A. Moore, A.L. Moore, D. Gust, J. Am. Chem. Soc. 128 (6) (2006) 1818;

(b) R.E. Palacios, S.L. Gould, C. Herrero, M. Hambourger, A. Brune, G. Kodis, P.A. Lidell, J. Kennis, A.N. Macpherson, D. Gust, T.A. Moore, A.L. Moore, Pure Appl. Chem. 77 (6) (2005) 1001.

[17] (a) K. Araki, H. Winnischofer, F.M. Engelmann, H.E. Toma, P. Losco, J. Porphyr. Phthaloc. 6 (1) (2002) 33;
(b) P.A. Anderson, F.R. Keene, T.J. Meyer, J.A. Moss, G.F. Strouse, J.A. Treadway, J. Chem. Soc., Dalton Trans. 20 (2002) 3820.

[18] (a) B.P. Sullivan, D.J. Salmon, T.J. Meyer, Inorg. Chem. 17 (12) (1978) 3334;
(b) J.A. Baumann, D.J. Salmon, S.T. Wilson, T.J. Meyer, W.E. Hatifield, Inorg. Chem. 17 (12) (1978) 3342;
(c) A.D. Adler, F.R. Longo, W. Shjergalis, J. Am. Chem. Soc. 86 (15) (1964) 3145.

[19] E.Z. Moreira, in: Synthesis and characterization of pentafluorophenyl-porphyrins substituted with ruthenium complexes, MS Thesis, São Paulo University, 2007.

[20] S.F. McClanahan, R.F. Dallinger, F.J. Holler, J.R. Kincard, J. Am. Chem. Soc. 107 (1985) 4853.

[21] E.R. Birnbaum, J.A. Hodge, M.W. Grinstaff, W.P. Schaefer, L. Henling, J.A. Labinger, J.E. Bercaw, H.B. Gray, Inorg. Chem. 34 (14) (1995) 3625.

[22] G.Z.G. Meng, B.R. James, K.A. Skov, Can. J. Chem. 72 (1994) 1894.

[23] T.P. Wijesekera, D. Dolphin, Metalloporphyrins in Catalytic Oxidations, Marcel Deker Inc., New York, 1994.

[24] V. Balzani, F. Scandola, in: Supramolecular Photochemistry, Ellis Horwood, Chichester, UK, 1991.

[25] M. Itou, M. Otake, Y. Araki, O. Ito, H. Kido, Inorg. Chem. 44 (5) (2005) 1580.

[26] J.C. Curtis, J.S. Berstein, T.J. Meyer, Inorg. Chem. 24 (1985) 385.